ARPA ORDER NO. 189-61

AD 625232

MEMORANDUM
RM-4732-ARPA
NOVEMBER 1965

SIMPLIFIED NORMAL MODE TREATMENT OF LONG-PERIOD ACOUSTIC-GRAVITY WAVES IN THE ATMOSPHERE

W. C. Meecham

PREPARED FOR:
ADVANCED RESEARCH PROJECTS AGENCY

The RAND Corporation
SANTA MONICA • CALIFORNIA

ARPA ORDER NO. 189-61

MEMORANDUM
RM-4732-ARPA
NOVEMBER 1965

SIMPLIFIED NORMAL MODE TREATMENT OF LONG-PERIOD ACOUSTIC-GRAVITY WAVES IN THE ATMOSPHERE

W. C. Meecham

This research is supported by the Advanced Research Projects Agency under Contract No. SD-79. Any views or conclusions contained in this Memorandum should not be interpreted as representing the official opinion or policy of ARPA.

DISTRIBUTION STATEMENT
Distribution of this document is unlimited.

The RAND Corporation
700 MAIN ST. • SANTA MONICA • CALIFORNIA • 90406

PREFACE

This Memorandum is a part of RAND's continuing VELA Analysis study for the Advanced Research Projects Agency and deals with a technique for detecting nuclear tests in the atmosphere. It presents the basic physical models for the infrasonic effects which have been observed from nuclear bursts. It discusses the propagation of low-frequency (less than one-tenth of a cycle per second) sound from nuclear explosions, attempting to predict the type of signal observed. For long-period waves, the Memorandum represents a refinement of previous work; for short-period waves, the Memorandum is perhaps the first serious examination of the problem in this context. This study should be of use in revealing more effective methods of data treatment to better evaluate the infrasonic method of detecting nuclear explosions.

The Memorandum was also submitted for publication in a special issue of the IEEE on high-altitude nuclear detection.

The author, a Consultant to The RAND Corporation, is a professor in the Department of Aeronautics and Engineering Mechanics, University of Minnesota.

SUMMARY

This Memorandum deals primarily with the effects of geometric dispersion on low-frequency mechanical waves generated by nuclear explosions. This dispersion is the result of the stratification of the atmosphere (to be distinguished from dispersion due to changes in physical characteristics due to changing frequency). It is found that the pressure signal can be divided naturally into an early-arriving acoustic-gravity portion (treated in this Memorandum) and a later--by about 5 per cent of the travel time--acoustic portion.

In general, both portions of the signal are inversely proportional to the range (geometric spreading included) although at very great ranges portions of the gravity wave fall off faster by $r^{1/6}$; the effect of dispersion is to reduce the signal by $r^{-\frac{1}{2}}$. Most of the signal is composed of many propagating modes which, at a given time and range, will each demonstrate a characteristic frequency. A simplified treatment of this complicated model picture is presented here. It is argued that a ray treatment for the higher-frequency portion is appropriate. It is shown that the frequency of the long-period signal increases with time. So long as the frequency of the received signal is less than the characteristic frequency of the initiating explosive impulse, it is found that the signal has a universal form for the fundamental mode. Such characteristics as yield, range, and phase velocity merely change the scaling of the signal. It is concluded that attenuation is probably not important for the low-frequency signals (below one cps) usually observed.

ACKNOWLEDGMENTS

It is a pleasure to acknowledge many very helpful discussions with Paul Tamarkin and T. F. Burke of The RAND Corporation.

CONTENTS

LIST OF FIGURES

I. INTRODUCTION

This Memorandum deals primarily with the effects of geometric dispersion on low-frequency mechanical waves generated by nuclear explosions. Geometric dispersion in general reduces the signal amplitude by an amount proportional to $r^{-\frac{1}{2}}$, where r is the range.(1) That this is so can be seen as follows: Suppose the amplitude of the wave train is A. The time duration of the disturbance after some time becomes proportional to the range as a result of dispersion. Total energy must be conserved (neglecting attenuation), so we have approximately

$$A^2 r = \text{constant}$$

Hence $A \sim r^{-\frac{1}{2}}$, as suggested. This reduction is in addition to that caused by geometric spreading.

The characteristics of low-frequency, atmospheric, acoustic-gravity waves have been investigated by a number of authors. Such waves can be generated by natural events as well as by nuclear explosions. We shall restrict the discussion largely to the latter. No attempt will be made here to compile a complete bibliography on the subject. However, we should mention normal mode calculations performed by Pfeffer,(2) Pfeffer and Zarichny,(3) Harkrider(4) and Pierce.(5) Harkrider has succeeded in calculating the expected low-frequency signal (hereafter this term, and the term long-period, mean waves with periods of more than one minute). He used five modes in the rather complex calculations. It is the major purpose of this Memorandum to attempt to obtain the essential characteristics of the low-frequency signal more simply (and, of course, less accurately).

The appropriate mathematical theory for the long-period characteristics of acoustic-gravity waves is given in Ref. 2. From the outset we distinguish between those waves for which gravitational effects are important (periods greater than 60 sec) and acoustic waves (periods less than about 60 sec). For the former, a normal mode treatment is indicated--as discussed in Refs. 2 through 5. We examine some of the expected characteristics of such waves on the basis of simplified models. For intermediate periods (from 30 to 120 sec) the situation is one where we must still use normal mode methods, but where a number of normal modes can propagate. For the acoustic part of the signal, a very great number of modes can propagate and a ray treatment is more useful.

We introduce here a discussion of the normal mode treatment. For our purpose it will be assumed that we observe the mode in the radiation zone, where kr >> 1, with k a typical propagation constant. Then we have for the pressure of the n^{th} mode

$$P_n = G(r)E_n(\omega, Z_o)\, E_n(\omega, Z)\, e^{ik_n(\omega)r - i\omega t} \tag{1}$$

where G(r) is a geometric spreading factor with

$$G(r) = r^{-\frac{1}{2}} \tag{2}$$

for propagation in a flat-earth atmosphere (see discussion below), E_n is the excitation function for point excitation,* Z_o is source height, Z is receiver height (set equal to zero for ground-level

*For details of the excitation process, see Ref. 4.

detection), $k_n = \omega/c_{pn}$, with c_{pn} the phase velocity of the n^{th} mode. It is assumed in Eq. (1) that the excitation is a single-frequency continuous wave. For the usual pulse excitation, we take the Fourier Transform (F.T.) of the initiating disturbance to find

$$P_n = \frac{G(r)}{2\pi} \int \overline{P}(\omega)\ E_n(\omega, Z_o)\ E_n(\omega, Z)\ e^{ik_n(\omega)r - i\omega t}\ d\omega \tag{3}$$

where we assume the excitation pressure $\overline{p}(t)$ has the F.T. $\overline{P}$

$$\overline{P}(\omega) = \int e^{i\omega t}\ \overline{p}(t)\ dt\,. \tag{4}$$

The function $\overline{p}(t)$ is found by taking the pressure at a range far enough from burst so that the overpressure is a small fraction of the ambient pressure, but not so far that the inhomogeneous characteristics of the medium influence the pulse form. Admittedly, it may be difficult to find such an intermediate range for large yield events. In such a case, we mean by $\overline{p}$ the linearized pressure disturbance which would be observed in an infinite homogeneous medium. The empirically observed form of the pressure is approximately[6]

$$\begin{aligned} \overline{p}(t) &= 0 && t < 0 \\ \overline{p}(t) &= p_o\left(1 - \frac{t}{t_+}\right) e^{-t/t_+} && t > 0 \end{aligned} \tag{5}$$

where $t_+ = Y^{1/3} t_1$, $t_1 \approx 1.0$ sec and Y is the yield in KT. The overpressure p_o is also proportional to $Y^{1/3}$. It is emphasized that the numerical value of t_+ is somewhat uncertain.* The F.T. of Eq. (5) is

$$\overline{P}(\omega) = p_o \frac{(-i\omega)}{(t_+^{-1} - i\omega)^2} \tag{6}$$

We discuss the calculations which are available for the functions appearing in Eq. (3). For simplicity the calculations have been performed assuming a horizontal atmosphere. This is adequate for ranges which are less than a quarter of the circumference of the earth. For greater ranges we should take into account the lack of further geometric spreading, due to the spherical earth. It seems reasonable to include, approximately, such effects by modifying the relation, Eq. (2), for the geometric factor. Thus, for the usual case where wavelengths are small compared with R_e, the radius of the earth, we have

$$G(r) = \left|R_e \sin \frac{r}{R_e}\right|^{-1/2} \tag{7}$$

with r measured along the surface of the earth. The focus at the antipode, $r = \pi R_e$, is smeared due to the fact that different earth paths have different temperatures and winds and thus different propagation times. The maximum value at the antipode is

*There are two, largely unresolved, difficulties in the determination of t_+. First, it might be that with a large burst, the first impulse takes on a nonspherical form before it becomes linearized, due to atmospheric inhomogeneities. In such a case it is necessary to use a source function more complicated than a simple source function. Second, the time of the positive phase, t_+, is not well known. In Ref. 6, p. 117, the value of t_+ has not attained its asymptotic value at the maximum range shown. On the basis of known information, this value must be estimated (the author is indebted to T. F. Burke of the RAND Corporation for this statement).

$$G_{anti}(r) \sim \frac{1}{(\alpha R_e)^{\frac{1}{2}}} \tag{8}$$

where α, order of a few per cent, is the fractional change in group velocity for different paths. Other effects aside, we see the focusing effect might be appreciable. An interesting consequence of Eq. (7) is that after traveling a fraction of the circumference of the earth, the signal shows no further reduction in amplitude due to geometric spreading. Observed reduction in signal amplitude with range then must be due to possible attenuation (usually negligible in situations of greatest practical interest) or dispersion, which is the main effect.

In order to correctly calculate the excitation functions and the modal phase velocities, c_{pn}, we must specify the atmospheric characteristics as a function of height. For this purpose Pfeffer and Zarichny[3] used the COSPAR standard atmosphere shown in Fig. 1. For a COSPAR atmosphere to 300 km (constant thereafter) they find the complicated phase and group velocity curves shown in Fig. 2 for the first few modes. In the same figure the results for a 52-km atmosphere (constant above 52 km) are shown. It is seen that this simpler model gives all of the characteristics of the 300-km model if attention is restricted to the nearly horizontal portions of the dispersion curves. This is true although the 52-km fundamental, for instance, is composed of portions of dispersion curves from several of the 300-km modes. It is seen that the major portion of the atmosphere (below 52 km) determines the propagation characteristics. For periods greater than 60 sec, it is seen that the 300-km atmosphere group velocity curves are either nearly horizontal or nearly vertical. The near-vertical

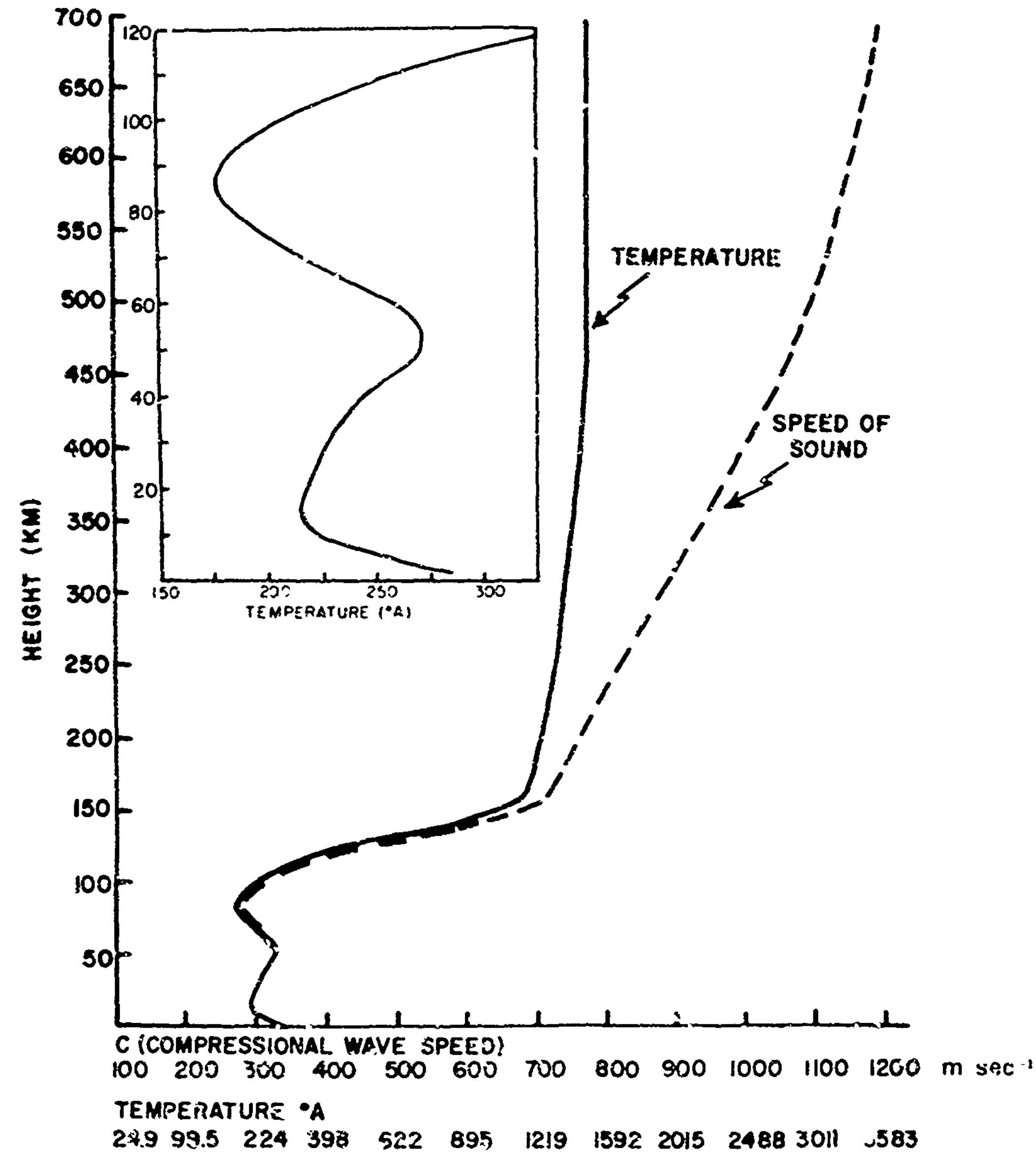

Fig. 1—Average vertical variation of absolute temperature in the atmosphere (estimated by the Comittee on Space Research; details up to 120 km given in insert. From Ref. 2)

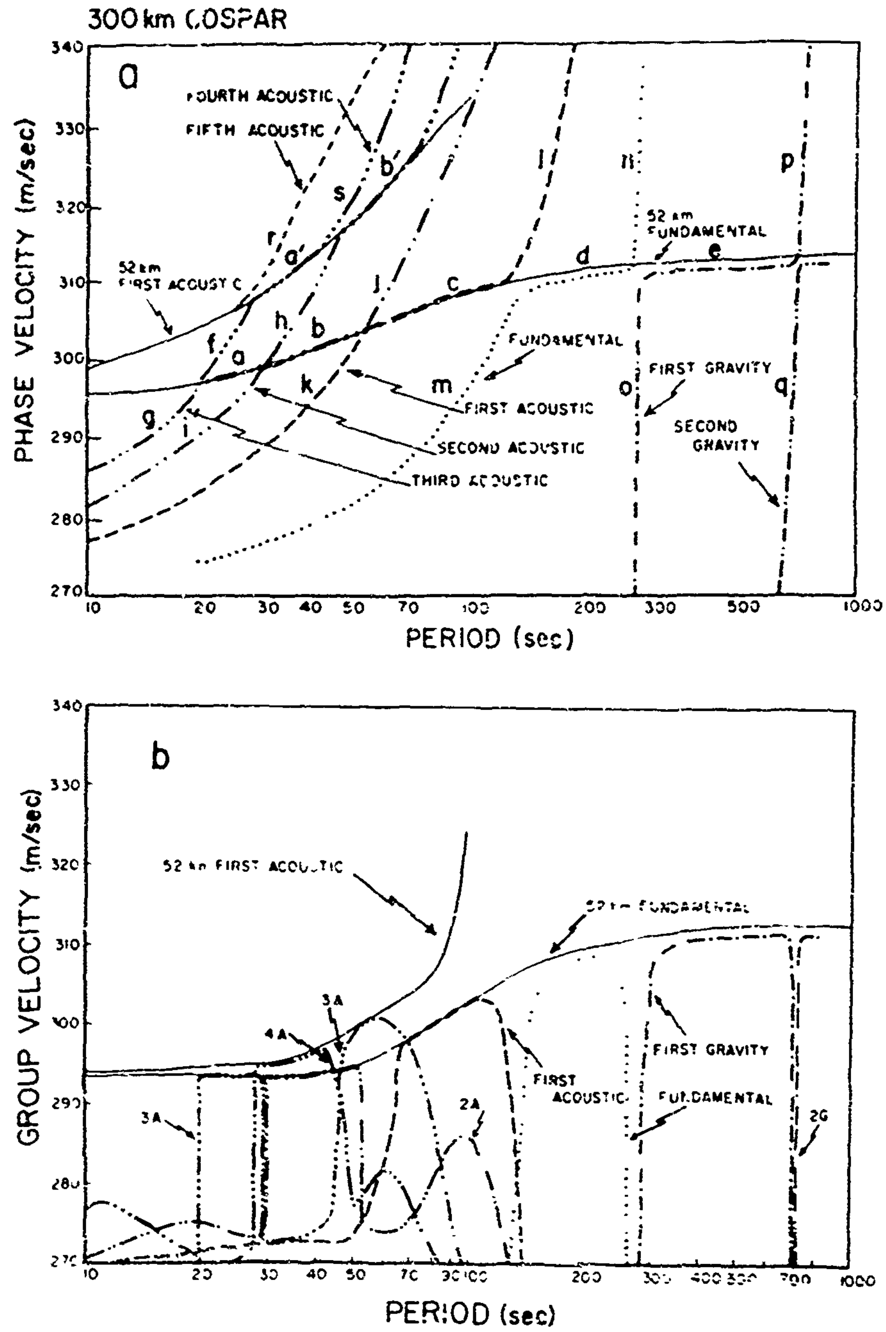

Fig.2—Phase and group velocity curves for COSPAR model atmospheres (From Ref.2)

portions contribute very little to the propagating signal. Consequently, there is at any given period only one principal propagating mode (and this one is very similar to the fundamental mode for the 52-km atmosphere). Of course, the propagating mode in fact comes from different modes of the 300-km atmosphere. For periods from somewhat above 30 sec to less than 60 sec we see that there are other contributing modes in the 300-km atmosphere. The important ones correspond to the fundamental and first acoustic modes for the 52-km atmosphere (there are presumably more than these two modes, although they were not calculated). As suggested above, these shorter-period modes (say, with periods less than 10 sec) are best treated as rays--which in fact are made up of a great many propagating modes. It should be pointed out that there may be doubts about the 300-km calculation discussed here. Tolstoy(7) has shown that there may be acoustic modes trapped at about 100 km between the upper-altitude temperature increase and the lower-altitude density increase. It is expected that such an effect will not influence the propagation of periods of interest here because of the attenuation at such altitudes.

It is interesting to note that the 52-km fundamental mode is made up of acoustic modes from the 300-km calculation for periods less than 250 sec and of gravity modes from the 300-km calculation for greater periods.

We shall in what follows generally restrict the discussion to the simpler dispersion curves taken from the calculations for the 52-km atmosphere. We see that the long-period gravitational contributions might be expected to arrive with a group velocity about 5 per cent greater (5 per cent less travel time) than the shorter-period acoustic signals. Of course, this observation applies to the quasihorizontal portions of the dispersion curves. The reader is referred to Refs. 2, 3 and 6 for more details concerning the normal mode calculations.

In the next section we shall simplify the problem by considering the behavior of a given normal mode at great ranges. It will be seen that, as sketched above, due to the dispersion caused by the stratified inhomogeneity of the atmosphere, the signal amplitude reduces with range. This and other characteristics of the signal will be obtained from Eq. (3). The discussion of possible attenuation effects appears in Section IV.

II. SIGNAL DISPERSION

For long-period, acoustic-gravity waves, we use the method of stationary phase to approximately evaluate Eq. (3). For large r and t, P and E_n are slowly varying functions of ω compared with the exponential. Then, following standard methods, we look for the stationary point of the argument of the exponential, which is seen to be ω_n given by

$$k_n'(\omega_n) \equiv c_{gn}^{-1} = \frac{t}{r} \qquad (9)$$

Here ω_n is the n^{th} mode frequency, if there is one, whose group velocity is equal to r/t. Then we have for that stationary contribution, at the frequency ω_n--given by Eq. (9)

$$P_n = G(r)e^{ik_n(\omega_n)r - i\omega_n t} E_n(\omega_n, Z_o) E_n(\omega_n, Z) \bar{P}(\omega_n) \times \left[\frac{i c_{gn}^2}{2\pi r c_{gn}'}\right]^{\frac{1}{2}} \qquad (10)$$

using

$$k_n'' = -\frac{c_{gn}'}{c_{gn}^2}, \qquad c_{gn}' \equiv \frac{d}{d\omega} c_{gn} \qquad (11)$$

obtained from Eq. (9). Equation (10) is valid in general when c'_{gn} is not too small (see condition Eq. (15)) and when the range is large, usually

$$k_n r \gg 1 \qquad (12)$$

The observed signal may be a sum of many modal contributions of the type given in Eq. (10). If $c'_{gn} \to 0$, as for instance when the period greatly exceeds 60 sec, we must modify the treatment. This is done next.

We note from Fig. 2 that for longer periods the 52-km fundamental phase and group velocities approach approximately constant values.* It is desirable to calculate the expected behavior for this situation. The first acoustic mode from the 52-km atmosphere can be treated using Eq. (10). We assume for long periods ($\omega \ll \omega_o$) for the fundamental mode, n = 0

$$k_o(\omega) \approx \frac{\omega}{c_{p\infty}} + \frac{\Delta c_p}{c_{p\infty}^2} \frac{\omega^3}{\omega_o^2} \tag{13}$$

with ω_o the transition frequency (about $2\pi/\tau_o$ where $\tau_o \approx 60$ sec) and

$$c_p \approx c_{p\infty} - \Delta c_p \left(\frac{\omega}{\omega_o}\right)^2 \tag{14}$$

where $c_{p\infty}$ is the phase velocity for very long periods and Δc_p is of the order of the change in the phase velocity, to be obtained by fitting the phase velocity of the fundamental 52-km mode in Fig. 2. We see from that figure that $\frac{\Delta c_p}{c_{p\infty}} \approx 0.05$.

The restriction on c'_{gn} for the validity of Eq. (10) can be written conveniently in terms of Eq. (14). It is

$$\frac{1}{6}\left(\frac{\omega_o}{\omega}\right)^{3/2}\left(\frac{\lambda_{o\infty}}{r}\right)^{1/2}\left(\frac{c_{p\infty}}{\Delta c_p}\right)^{1/2} \ll 1 \tag{15}$$

*It might be thought from a casual observation of Fig. 2 that there is a similar situation for short periods. However, when the curves are put on a linear rather than a logarithmic plot, it is found that they actually have finite slope as the period tends to zero.

with $\lambda_{o\infty}$ the wavelength corresponding to $c_{p\infty}$. For values taken from Fig. 2, the left side of Eq. (15) is .02 for a range of 8000 km; for most ranges of interest Eq. (15) is fulfilled.

From Eqs. (5) and (6) note that for ordinary yields Y, the condition that $\omega \ll \omega_o$ implies that we need the low-frequency limit behavior of $\overline{P}$ in Eq. (3). From Eq. (6) we see

$$\overline{P} \approx p_o t^2(-i\omega), \qquad \omega \ll t_+^{-1} \tag{16}$$

Similarly, it is reasonable to believe (and calculations in Ref. 4 show) that the characteristic frequencies of E_o are of order ω_o. Then we also need the long-period behavior of E_o, seen to be approximately constant;* this value of E_o is called E_{LP} below. Substituting these low-frequency approximations in Eq. (3) we find

$$P_{o,LP} = G(r)\ p_o t_+^2\ E_{LP}(Z)\ E_{LP}(Z_o)\ \frac{d}{dt}\ I_{LP} \tag{17}$$

with

$$I_{LP} \equiv \frac{1}{2\pi} \int \exp\ i\left\{\left[\frac{\omega}{c_{p\infty}} + \frac{\Delta c_p}{c_{p\infty}^2}\frac{\omega^3}{\omega_o^2}\right]r - \omega t\right\} d\omega \tag{18}$$

I_{LP} (the response to a delta function excitation) is found by standard methods to be

---

*See p. 5309 of Ref. 4.

$$I_{LP} = \begin{cases} \frac{1}{3\pi\tau}\left[\frac{1}{\tau}\left(\frac{r}{c_{p\infty}} - t\right)\right]^{1/2} K_{\frac{1}{3}}\left(2\left[\frac{\left(\frac{r}{c_{p\infty}} - t\right)}{3\tau}\right]^{3/2}\right), & \frac{r}{c_{p\infty}} - t > 0 \\ \frac{1}{3\sqrt{3}}\left[\frac{1}{\tau}\left(t - \frac{r}{c_{p\infty}}\right)\right]^{1/2} \left\{J_{\frac{1}{3}}\left(2\left[\frac{1}{3\tau}\left(t - \frac{r}{c_{p\infty}}\right)\right]^{3/2}\right)\right. & \\ \left. + J_{-\frac{1}{3}}\left(2\left[\frac{1}{3\tau}\left(t - \frac{r}{c_{p\infty}}\right)\right]^{3/2}\right)\right\} & t - \frac{r}{c_{p\infty}} > 0 \end{cases} \tag{19}$$

with

$$\tau \equiv \left(\frac{\Delta c_p}{c_{p\infty}^2} \frac{r}{\omega_o^2}\right)^{1/3} \tag{20}$$

Here $J_{1/3}$ and $K_{1/3}$ are the usual Bessel and modified Bessel functions. It is easily seen from Eq. (18) that τ^{-1} is the order of the value of ω for which

$$\frac{\Delta c_p}{c_{p\infty}^2} \frac{\omega^3}{\omega_o^2} r \sim 1 \tag{21}$$

that is, where the cubic term in the exponential begins to bring about convergence of the integral. The error made by using the low-frequency approximation for $\overline{P}(\omega)$ in the region $\omega > t_+^{-1}$ is negligible if

$$\left(\frac{c_{p\infty}^2}{\Delta c_p r \omega_o}\right)^{2/3} << 1$$

This condition is satisfied for ranges exceeding a hundred kilometers. The result of Eqs. (17) through (20) shows that the medium is essentially a low-pass filter for long-period waves when there is concern only with the most important mode, the fundamental.

III. DISCUSSION OF LONG- AND INTERMEDIATE-PERIOD SIGNAL DISPERSION

The reader is reminded that here long periods are those over 60 sec and intermediate periods are those between about 30 and 120 sec. Under the assumption that for long periods the fundamental mode has group and phase velocities which are nearly constant, the result given in Eqs. (17)-(20) was obtained. The following characteristics appear from Eqs. (17)-(20) for the early long-period component--sometimes called the gravity wave:

1. The signal arrival time is approximately fixed by the long-period phase velocity, $c_{p\infty}$. The precursor at earlier times increases in amplitude exponentially. The signal amplitude then, after this "crescendo," increases like $\left(\frac{\Delta t}{\tau}\right)^{\frac{1}{4}}$, where $\Delta t = t - \frac{r}{c_{p\infty}}$. This increase in amplitude continues until $\Delta t \gtrsim 3\tau^3 \, t_+^{-2}$, when frequencies are such that the approximation, Eq. (16), fails. For later times the more general result given in Eq. (10) could be used (see below). Since the growth in signal amplitude is due to the increase of $\overline{P}(\omega)$ with ω, an alternative procedure can be used. We use the pulse transform, Eq. (6), and the period as a function of $\frac{\Delta t}{\tau}$ given in Eq. (22) to approximately correct for the pulse form. For this purpose, multiply Eq. (19) by

$$\left[1 + \left(\frac{t_+}{\tau}\right)^2 \frac{\Delta t}{3\tau}\right]^{-1} \tag{21a}$$

We assume in such a treatment that the approximate effect of the pulse spectrum is to multiply the signal at time Δt by the value of the spectrum function appropriate to the frequency occurring at that time.

2. The first important signal arrival, when $t \approx r/c_{pm}$, has a long period followed by successively shorter-period arrivals (normal dispersion). From Eq. (19) it is seen that using πn for the approximate zeros of the Bessel functions, when $(\Delta t/\tau)^{3/2} > 1$, the period for signal delayed by Δt is

$$T \approx 2\pi \left(\frac{3\tau^3}{\Delta t}\right)^{\frac{1}{2}} \tag{22}$$

We see the period decreases like the $\frac{1}{2}$ power of the delay in this normally dispersed part of the signal.

3. The range dependence is interesting. The amplitude of the early part of the low-frequency signal is seen from Eqs. (17)-(20) to fall off like the 2/3 power of the range due to dispersion (remembering to take the derivative as in Eq. (17)). For ranges considerably less than R_e, we use Eq. (3) for the function G and find that the long-period wave should decrease in amplitude like $r^{-7/6}$. For greater ranges, $r \gtrsim R_e$, the dependence is roughly like $r^{-2/3}$. The period of the first arrival, at a given Δt, increases like $r^{\frac{1}{2}}$ according to Eq. (22). As the range increases, the amplitude decreases and the period increases due to dispersion. Relatively slow decreases in amplitude with range have been found experimentally for signals which circle the globe.(8-9)

4. From Eq. (17) and the scaling laws discussed in Section I, we see that the amplitude is proportional to yield. The signal waveform is otherwise independent of yield so long

as $\Delta t < 3\tau^3 t_+^{-2}$. This should be true for the long-period gravity wave, but care must be used when the delay is such that the wave merges with the shorter-period components.

5. For $\Delta t < 3\tau^3 t_+^{-2}$, so that $\omega < t_+^{-1}$, we see the signal has a universal form. The yield, range, and atmospheric effects enter the scale of the amplitude (for yield) and the time scale (for range and atmospheric effects).

These characteristics are also obtainable using the simple stationary phase treatment given by Eq. (10). It is emphasized that this result applies only to the fundamental mode (as defined for the 52-km atmosphere). Often one or more of the higher modes can be expected to appear also, and this effect must be calculated using Eqs. (9)-(10).

Consider an example: $r = 10^4$ km, $\omega_o = 2\pi/60$, $\frac{\Delta c_p}{c_{p\infty}} = .05$, $c_{p\infty} = \frac{1}{3}$ km/sec. Then we find $\tau \approx 50$ sec. Accordingly, the result, Eqs. (17)-(20), is valid for $\Delta t < 3\tau^3 t_+^{-2}$; and with Y = 4 MT, $t_+ = 16$ sec, we need $\Delta t < 24$ min. From Eq. (22) for $\Delta t = 10^3$ sec, the period, T, is 115 sec; for $\Delta t = 4000$, $T \approx 55$ sec.

The universal result, Eqs. (17)-(20), is shown in Fig. 3. There the quantity $\tau^2 \frac{d}{dt} I_{LP}\left(\frac{\Delta t}{\tau}\right)$ is plotted. The characteristics, discussed above, can be seen. The dashed envelope curve gives the approximate modification due to a 4-MT pulse form, given by the factor of Eq. (21a) (parameters for this curve are those of the example just completed). It is interesting to note that the initiation of the signal using the velocity $c_{p\infty}$ is correctly measured from the first positive maximum. The precursor ($\Delta t < 0$) is not actually in conflict

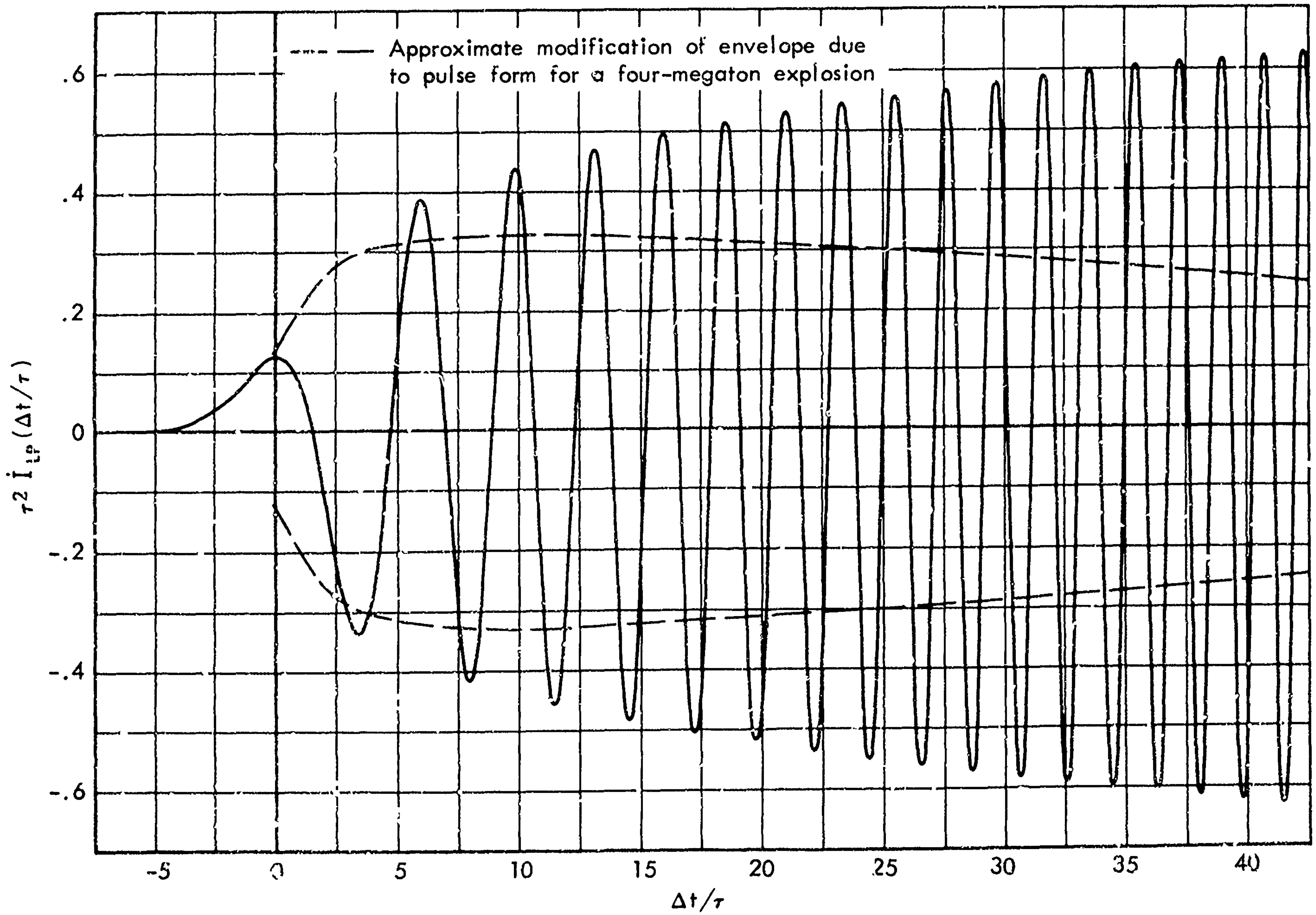

Fig. 3—Low-frequency universal response of the atmosphere for the fundamental mode

with the general theorems[10] concerning the velocity of propagation of the signal wave front because of the form of the dispersion curve. We should use Eqs. (9)-(10) to calculate the curve when $\frac{\Delta t}{\tau}$ is such that $\omega \geq \omega_o$; for the example above (4 MT) this means for periods of about one in the dimensionless units of the graph. However, the approximation, Eq. (13), is not bad for much higher frequencies, so that it is not unreasonable to accept the results for greater time delay.

We turn now to a discussion of the intermediate periods (periods between 30 and 120 sec). We use Eq. (10) and in general we must consider many propagating modes in the signal. The number of modes may be quite large when the period is much less than 60 sec. We see the following characteristics for the intermediate component:

1. By referring to Ref. 4,* it is found that the fundamental mode for periods greater than 90 sec has an excitation function which is constant at an altitude of 18.5 km. More work needs to be done on the excitation functions in order that the frequency dependence may be examined more closely. As already remarked, we assume that for periods greater than 60 sec the excitation functions are constant.
2. Other things being equal, the amplitude of the n^{th} mode is inversely proportional to the square root of the slope of the modal group velocity for the frequency in question. As suggested above, the most important modes are those whose group velocity curves are most nearly horizontal (see Eq. (10)).
3. The general characteristics of the signal are determined as follows (see sketch below which is a schematic representa-

*See p. 5309 of Ref. 4.

tion of the first three modes). First, for a given range and time, Eq. (9) is used to determine the appropriate group velocity. Then the lower curves for 52-km atmosphere are used from Fig. 2 to find which periods appear for the various modes. Unfortunately, the calculations given there are only for the fundamental and the first acoustic modes. The other acoustic modes must be imagined as lying above the first. The slope of the group velocity curve is determined from the calculation. The result is that for any range and time there can be a great number of modes arriving, each with its appropriate period as explained. We see in the sketch the three periods for the first three acoustic modes at r,t. Others are not shown. At a given time many different modes, each with its own frequency, will make up the signal, though the fundamental mode is dominant for low frequencies.

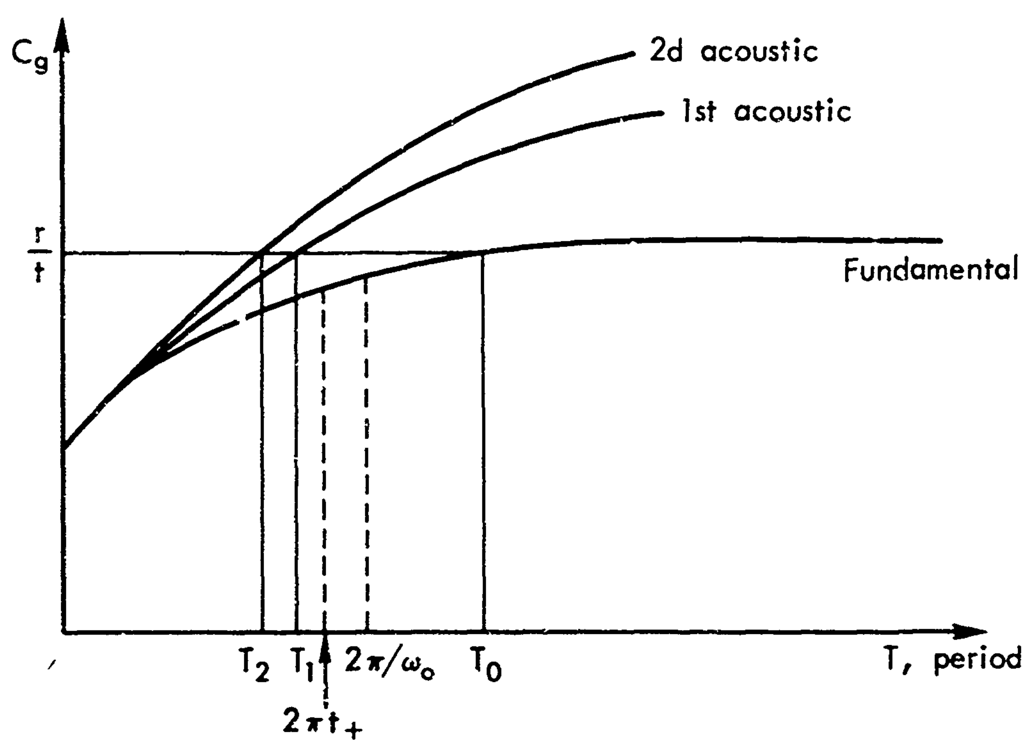

4. The periods of the various modes decrease as the time of observation increases (normal dispersion), as can be seen from the sketch. Normal dispersion is (usually) observed experimentally.[8,9,11] The characteristic empirical period, $2\pi\omega_0^{-1}$, is shown in the sketch. The period for which the pulse form becomes important, $2\pi t_+$, is also shown; it is the period below which the simple form of the fundamental, Eqs. (17)-(20), must be modified because of pulse form.

5. The amplitude of the signal falls off like $r^{-\frac{1}{2}}$ due to dispersion. For ranges less than R_e there is an additional factor of $r^{-\frac{1}{2}}$ for geometric spreading, giving an inverse r amplitude dependence which is apparently spherical. This amplitude reduction with range is (approximately) observed experimentally. For instance, if we suppose that the pressure wave from a 1-MT nuclear explosion drops to one-tenth ambient pressure at a range of about 10 km, we find for the overpressure at 10,000 km from the above

$$P_{10,000} = \frac{(0.1)10^6}{(10^4/10)} = 100 \text{ d cm}^{-2} \tag{23}$$

This is the approximate size of observed signals.[11] It is interesting to note that without dispersion, signals would be 30 times the value given in Eq. (23), i.e., much larger than signals are found to be from such events. We note from Eqs. (10) and (18)-(20) that the long-period, fundamental gravity wave falls off faster with range (by $r^{-1/6}$) than the intermediate- (or short-) period wave.

6. The most prominent frequency in the intermediate signal cannot be determined without knowledge of the excitation functions. For short periods where a ray treatment applies, we may expect the signal to show a frequency maximum at that of the pulse maximum, $\omega_{max} = t_+^{-1}$. Hence, the "frequency" of the signal would be proportional to $Y^{1/3}$.

7. From Eqs. (6) and (10) it is expected that the amplitude of the signal would be proportional to p_o, that is, proportional to $Y^{1/3}$. However, the excitation function can indirectly, through the parameter t_+ in $\overline{P}$, influence the dependence of the amplitude upon yield. The <u>acoustic</u> signal amplitude can, of course, be influenced by fluctuating atmospheric propagation characteristics.

Before closing this section, it is useful to express the intermediate-period mode results in terms of the power spectrum function. We use the definition of the power spectrum for a segment, $2T_o$, of record f(t)

$$P.S.(\omega) = \frac{\pi}{T_o} \left| A_{T_o}(\omega) \right|^2 \tag{24}$$

with

$$A_{T_o}(\omega) \equiv \frac{1}{2\pi} \int_{-T_o}^{T_o} e^{-i\omega t} f(t)\, dt. \tag{25}$$

The result for the power spectrum of the n^{th} mode is found from Eqs. (10) and (24) to be

$$P.S._n(\omega) = \frac{G^2(r)}{r} \left| E_n(\omega_n, Z_o)\, E_n(\omega_n, Z)\, \bar{P}\,(\omega_n) \right|^2 \cdot \frac{C_{gn}^2}{8\pi^2\, c'_{gn}} \left(\frac{\sin^2 T_o\,(\omega-\omega_n)}{(\omega-\omega_n)^2\, T_o} \right) \tag{26}$$

We assume that the change in ω_n is slight in the record segment time T_o. The last factor in Eq. (26) gives the peak width when it is determined by T_o. The total power spectrum is approximately a sum of terms like Eq. (26), one for each mode.

It is also useful to consider the total energy in the n^{th} mode for $r < R_e$

$$\mathcal{E}_n = K \int_0^{2\pi} r\, d\theta \int_0^{\infty} dZ \int |P_n|^2\, dt \tag{27}$$

where K is constant, independent of range, and θ is the azimuth angle about the source. The result must be independent of the range for a loss-free medium. The total energy is given by a sum over terms like Eq. (27), covering all of the propagating modes; we neglect interference effects which do not affect the energy content. The range independence is, of course, a reflection of the fact that geometric dispersion in the medium does not affect the energy of the propagating wave. This suggests using the integral of the square of the observed pressure signal since this quantity would show no reduction with range due to dispersion. It would decrease like $1/r$ rather than $1/r^2$. The range dependence of the energy would be entirely geometric. For $r > R_e$, the average geometric reduction should be slight. For such ranges, we should find

$$\int p^2(t)\, dt \cong \text{constant, independent of } r \qquad (28)$$

Noise can be removed by subtracting an integral like Eq. (28) for the noise signal. It should be emphasized that Eq. (28), representing as it does a fraction of the explosion energy, should be proportional to yield. This dependence should be compared with the fractional power yield dependence of some other characteristics. We see from Eq. (28), as remarked above, that since dispersion causes the signal to spread in time proportional to range, we can expect the pressure to be proportional to $r^{-\frac{1}{2}}$ for ranges such that $r > R_e$.

For shorter-period acoustic waves, we can employ the full formalism of ray treatment. This will not be done here. However, a few outstanding characteristics are worth noting. First, the range dependence due to atmospheric stratification is also $r^{-\frac{1}{2}}$ as for normal modes. We might expect interference effects due to multi-path phenomena for shorter ranges. The most prominent circular frequency in this part of the signal will occur at $(t^{+})^{-1}$, the characteristic frequency of the initiating explosion.

IV. SIGNAL ATTENUATION

We shall consider in this section a few of the more prominent attenuation mechanisms. First, we examine absorption due to molecular, vibrational relaxation. Using accepted values we have for the attenuation coefficient

$$\alpha \sim 10^{-9} \frac{\omega^2 \tau}{1 + \omega^2 \tau^2} \ \mathrm{cm}^{-1}, \ \tau \approx .002 - .05 \ \mathrm{sec} \tag{29}$$

For $\omega = \frac{2\pi}{5}$, a 5-sec period

$$\alpha \sim 10^{-11} \ \mathrm{cm}^{-1} \tag{30}$$

The signal reduces to a fraction of its value in 10^6 km due to molecular absorption. For periods above a few seconds we conclude that such attenuation can be neglected.

Consider now the attenuation which would be caused by scattering from velocity irregularities set up by atmospheric turbulence. Due to the pulsed nature of the initiating signal, we shall for simplicity assume that once a signal is scattered it is lost. It is true that some of such energy is regained, but for the present purpose of estimation we neglect such contributions. Since we are interested here in long-period disturbances whose wavelengths are usually greater than the scale of atmospheric irregularities, we restrict the discussion to Rayleigh scattering. We find for the attenuation coefficient

$$\alpha \sim (ka)^4 \frac{1}{a} (\Delta N)^2, \ ka < 1 \tag{31}$$

$$\sim \frac{1}{a} (\Delta N)^2, \qquad ka \gtrsim 1 \tag{32}$$

(Eq. (32) is given for completeness.)

In Eq. (31), a is the turbulence scale length--the correlation length, ΔN is the turbulent velocity fluctuation relative to the speed of sound, and we have assumed that the turbulent eddies are "close-packed," that is, the medium is fully irregular. The Rayleigh result goes over to a geometrical optics result of the order given in Eq. (32) for higher frequencies. A typical scale length for atmospheric turbulence is about 1 km. Taking the maximum attenuation given in Eq. (32), for a period less than about 20 sec, and using $\Delta N \simeq .005$, a value appropriate to the upper atmosphere, we find

$$\alpha^{-1} \sim 40,000 \text{ km}$$

Longer periods would give even less attenuation. We conclude that because of the low contrast of turbulent velocity fluctuations, attenuation due to such scattering is negligible for low-frequency waves.

For higher frequencies, although the scattering from turbulent eddies is slight, there can be appreciable reflection from laminar wind ducts.

More generally, it can be argued from experimental observations (see, for instance, Refs. 8 and 9) that there is no appreciable signal attenuation at present ranges of observation. Any attenuation mechanism would give a certain reduction in signal per unit length. Then, if the signal is reduced by attenuation to a fraction by traveling a fraction of the way around the earth, it would be reduced by that fraction to the n^{th} power for a path n times as long. But the first reduction due to attenuation must be negligible since no such drastic reduction is observed in subsequent passes around the earth.

V. CONCLUSIONS

We have examined the effect of dispersion on acoustic-gravity waves generated by nuclear events at great ranges. It is shown by using the normal mode calculations of Pfeffer that it is natural to divide the signal into three parts: low-frequency gravity modes, intermediate-frequency signals, and acoustic signals. The characteristics of the first two were examined in Sections II and III. It is found that, in general, dispersion causes a reduction of signal amplitude proportional to the square root of the range, regardless of the portion of the signal considered. This is in addition to the reduction due to simple geometric spreading. The additional range dependence is sufficient to give the observed reduction in signal level over that expected from ordinary cylindrical spreading.

We summarize the results. In order to calculate the pressure in different period ranges (alternatively for different time delays), see below.

Fundamental Mode

- For a period greater than $\frac{2\pi}{\omega_o} = 60$ sec and $2\pi\, t_+$ (alternatively Δt less than $3 \frac{\Delta c_p}{c_{p\infty}^2} r$ and $3 \frac{\Delta c_p}{c_{p\infty}^2} \frac{r}{\omega_o^2 t_+^2}$) use Eqs. (17)-(20), where it is assumed the excitation function is constant in frequency.
- For a period less than either above (alternatively Δt greater than corresponding quantities above), use Eqs. (9)-(10).

Higher Modes

- For all period use Eqs. (9)-(10).

It is appropriate to comment on the expected variability of pressure records. First, it seems reasonable to assume that the gravity waves will exhibit little variability with changes in tropospheric conditions, since they have very great wavelengths. The same cannot be said of the acoustic waves (periods less than about 20 sec). Their wavelengths are of the order of, or less than, the size of prominent features of the lower atmosphere. From Fig. 1 it is seen that there is an acoustic velocity maximum at about 50 km. This maximum has a width of about 10 km, which corresponds to the wavelength of a 30-sec period wave. For such periods and shorter, we should expect that changes in wind velocity at 50 km might seriously affect the modal excitation functions and to a lesser extent the dispersion curves, or alternatively the ray propagation characteristics. In this way, the large and variable winds at such altitudes might cause considerable variability in the acoustic and perhaps intermediate-frequency signals. This would be particularly true since relatively small changes in wind speed are seen from Fig. 1 to be sufficient to cause the disappearance of the lower duct altogether, as observed from the ground.

Another conclusion which should be emphasized is that the integral of the square of pressure record, the "energy" in the wave, may serve as a more sensitive characteristic for detection than the signal itself. This is so since such a measure removes the effect of dispersion. Thus, the range dependence is just that of the (range periodic) geometric spreading. It is seen that this energy is proportional to yield.

For future work it is suggested that power spectral functions (P.S.F.'s) be calculated for the signal records in order to determine the signal characteristics along the lines discussed in this Memorandum.

Signal variability forms an interesting topic in itself. It would be helpful to attempt to correlate this variability with upper atmosphere winds. It will be interesting to examine further P.S.F.'s to see the behavior of the spectral peaks. In particular, the reduction in frequency with increased time of travel should be looked for. Such frequency-travel time results can be used to obtain an experimental determination of the group velocity dispersion curves for the various modes. Finally, it seems desirable to obtain the characteristics of the modal excitation functions for shorter periods and as a function of altitude. It is noted that these functions may yield important information on burst height (see Eq. (1)).

The results of the simplified calculations discussed in this report have been compared with the more complete results of Harkrider.[4] The frequency dispersion and signal amplitudes correspond well, within 10-20 per cent in the cases considered.

REFERENCES

1. Latter, R., R. F. Herbst, and K. M. Watson, Annual Review of Nuclear Science, Vol. 11, 1961, pp. 371-418.

2. Pfeffer, R. L., J. Atmos. Sci., Vol. 19, 1962, pp. 251-255.

3. Pfeffer, R. L., and J. Zarichny, Geofisica Pura E Applicata-Milano, Vol. 55, 1963/II, pp. 175-199.

4. Harkrider, D. G., J. Geophys. Res., Vol. 69, 1964, pp. 5295-5321.

5. Pierce, A. D., Propagation of Acoustic-Gravity Waves from a Small Source Above the Ground in an Isothermal Atmosphere, The RAND Corporation, RM-3596, May 1963.

6. Glasstone, S. (ed.), The Effects of Nuclear Weapons, U. S. Government Printing Office, Washington, D. C., June 1957.

7. Tolstoy, Ivan, Rev. Mod. Phys., Vol. 35, 1963, pp. 207-230.

8. Donn, W. L., and M. Ewing, J. Atmos. Sci., Vol. 19, 1962, pp. 264-273.

9. Jones, R. V., Nature, Vol. 193, 1962, pp. 229-232.

10. Stratton, J. A., Electromagnetic Theory, McGraw-Hill Book Company, New York, 1941, pp. 333ff.

11. Hunt, J. N., R. Palmer, and Sir W. Penney, Phil. Trans. Roy. Soc. (London), Vol. A252, 1960, pp. 275-315.

DOCUMENT CONTROL DATA

1. ORIGINATING ACTIVITY THE RAND CORPORATION	2a. REPORT SECURITY CLASSIFICATION UNCLASSIFIED 2b. GROUP
3. REPORT TITLE SIMPLIFIED NORMAL MODE TREATMENT OF LONG-PERIOD ACOUSTIC-GRAVITY WAVES IN THE ATMOSPHERE	
4. AUTHOR(S) (Last name, first name, initial) Meecham, W. C.	

5. REPORT DATE	6a. TOTAL NO. OF PAGES	6b. NO. OF REFS.
November 1965	41	11

7. CONTRACT or GRANT NO.	8. ORIGINATOR'S REPORT NO.
SD-79	RM-4732-ARPA

9a. AVAILABILITY/LIMITATION NOTICES	9b. SPONSORING AGENCY
	Advanced Research Projects Agency

10. ABSTRACT

A discussion of the effects of geometric dispersion due to stratification of the atmosphere on low-frequency mechanical waves generated by nuclear explosions. It is found that the pressure signal can be divided naturally into an early-arriving acoustic-gravity portion and a later acoustic portion, both portions being inversely proportional to the range (geometric spreading included). At very great ranges, however, portions of the gravity wave fall off faster by $r^{1/6}$; the effect of dispersion is to reduce the signal by $r^{-1/2}$. Most of the signal is composed of many propagating modes which, at a given range and time, will each demonstrate a characteristic frequency. A simplified treatment of the model picture is presented, along with the argument that a ray treatment for the high-frequency portion is appropriate. 41 pp. Illus.

11. KEY WORDS

Atmosphere
Waves
Nuclear blasts
Physics
Signals